ELSEVIER

Journal of Molecular Catalysis A: Chemical 103 (1995) 105–116

JOURNAL OF MOLECULAR CATALYSIS A: CHEMICAL

The effect of iron on the activity and the selectivity of Rh/ZrO_2 catalysts in the CO hydrogenation

E. Guglielminotti [a], F. Pinna [b], M. Rigoni [b], G. Strukul [b], L. Zanderighi [c,*]

[a] *Dipartimento di Chimica Inorganica, Chimica Fisica e dei Materiali, Università di Torino, Via P. Giuria 7, 10125 Torino, Italy*

[b] *Dipartimento di Chimica, Università di Venezia, Dorsoduro 2137, 30123 Venezia, Italy*

[c] *Dipartimento di Chimica Fisica ed Elettrochimica, Università di Milano, Via Golgi 19, 20133 Milano, Italy*

Received 3 February 1995; revised 16 May 1995

Abstract

Rh/ZrO_2 catalysts (1% w/w) with different amounts of iron as promoter (Fe/Rh atomic ratio in the range 0–2) were prepared from three precursors: carbonyl clusters, chloride salts, nitrate salts. The catalysts were characterized by H_2 and O_2 chemisorption, titration of chemisorbed oxygen with hydrogen, TPR, X-ray analysis and IR spectroscopy of chemisorbed CO in the range of 300–773 K. The activity has been tested in the CO hydrogenation reaction ($H_2/CO = 3/1$) at 493 K under atmospheric pressure. The physico-chemical characterization of the catalysts evidenced that iron is present either as oxidized $Fe^{\delta+}$ or in the reduced Fe^0 form: IR analysis revealed that some reduced iron either decorates or is near the border of Rh particles. The metal precursors do not seem to influence significantly the behaviour of the catalysts. Two opposing effects of iron were evidenced: (i) a decrease of Rh sites available for carbon monoxide and hydrogen chemisorption; (ii) an increase of doubly bonded CO (Rh–CO–Fe) favoured by Fe^{x+} sites, contiguous to Rh sites, that are reduced to Fe^0 sites in reaction conditions. Depending on the surface environment, the bridged CO may dissociate to Rh–C and Fe–O or insert a hydrogen or an alkyl group with formation of an acyl species.

Keywords: Carbon monoxide; Hydrogenation; Iron; Rhodium; Selectivity; Zirconium

1. Introduction

In previous papers we reported the results of CO/H_2 reaction on Rh/ZrO_2 catalysts, prepared from Rh carbonyl clusters both on pure ZrO_2 and in the presence of additives [1,2].

Rh/ZrO_2 unpromoted catalysts [1] show a good activity and selectivity to oxygenates, mainly to ethanol [3]. The activity decreases by increasing the temperature of the thermal pretreatment in hydrogen stream, owing to the increase of the metal support interaction, due to a partial migration of zirconia over rhodium particles, as shown by the decrease of the chemisorption of CO and H_2 [1].

Catalyst additives for CO hydrogenation reaction have been classified as 'oxophilic' and 'basic' according to Sachtler and Ichikawa [4]. The first category includes MoO_3, MnO_2, Ti_2O_3, ZrO_2, etc. and promotes the CO conversion and the selectivity to oxygenates. On the other hand 'basic' oxides, such as Fe_2O_3, ZnO, etc., increase the selectivity to oxygenates while having a very small effect on the activity [5].

* Corresponding author.

1381-1169/95/$09.50 © 1995 Elsevier Science B.V. All rights reserved
SSDI 1381-1169(95)00119-0

We have tested the effect of Mo addition on the Rh/ZrO_2 catalysts [6]: in agreement with other authors [7,8] Mo increases both the activity and the selectivity to oxygenates. Moreover it has been possible to evidence an interaction between rhodium and molybdenum and to define some elementary steps in CO hydrogenation.

According to Ichikawa, iron is a very good promoter of Rh, Pt, Pd on SiO_2 catalysts for the CO conversion to alcohols [9].

More recently Somorjai et al. [10] have studied the influence of the Lewis acidity of some metal oxides (AlO_x, TiO_x, VO_x, FeO_x, ZrO_x, MbO_x, TaO_x and WO_x) on the hydrogenation activity of polycrystalline Rh foil. With AlO_x and FeO_x a decrease in the rate of methane formation has been observed.

In order to exploit the potential utility of the Rh/ZrO_2 catalysts for CO hydrogenation, in this work we report the use of 'basic' Fe promoter, that complements our previous studies in this field.

Table 1
Analytical data of the catalysts reduced at 523 K

Catalysts	w/w Rh (%)	w/w Fe (%)	Fe/Rh atomic ratio
Rh(CO)	1.0	–	0.0
Rh–Fe(CO)	0.99	0.26	0.48
Rh–Fe(CO)	0.99	0.43	0.80
Rh–Fe(CO)	1.01	0.57	1.06
Fe(CO)	–	0.52	–
Rh(Cl)	1.09	–	0.0
Rh–Fe(Cl)	1.23	0.42	0.63
Rh–Fe(Cl)	0.82	0.58	1.30
Rh–Fe(Cl)	1.00	0.79	1.42
Rh–Fe(Cl)	0.90	1.69	3.46
Rh(Cl)	1.09	–	–
RhFe(Cl)	0.83	0.30	0.67
RhFe(Cl)	0.75	0.52	1.27
RhFe(Cl)	0.82	0.57	1.28
RhFe(Cl)	1.21	1.63	2.49
Fe(Cl)	–	2.50	–
Rh(N)	1.03	–	0.0
RhFe(N)	1.36	0.46	0.62
RhFe(N)	0.89	0.86	1.40
RhFe(N)	0.88	0.98	1.90
RhFe(N)	1.39	1.43	2.00
Fe(N)	–	2.48	–

Rh–Fe two-stage impregnation; RhFe co-impregnation. (CO) from carbonyl clusters; (Cl) from chloride salts; (N) from nitrate salts.

2. Experimental

2.1. Catalyst preparation

Zirconium oxide was prepared by dropping a 10% ammonia solution into a water solution of $ZrOCl_2 \cdot 8H_2O$ (Riedel), with stirring, until pH = 10 was reached. The precipitated zirconium hydroxide, after filtration, was washed, under stirring, with a warm (313 K) diluted (pH 8–9) ammonia solution until the disappearance of chloride ions. Finally, the zirconium hydroxide was dried in an oven at 383 K for 18 h. The hydroxide was transformed into zirconium oxide by heating in a fluidized bed at 773 K for 2 h in a stream of air (40 ml/min). Surface area and crystalline phase composition of the support were determined by BET and X-ray diffraction analysis respectively. The catalysts were prepared by supporting various precursors, such as carbonyl clusters, chloride or nitrate salts, on the previously prepared zirconium oxide.

Supported Rh carbonyl clusters were prepared by adding dropwise a solution of $Rh_4(CO)_{12}$ (Fluka) in heptane to a suspension of ZrO_2 under stirring. The same procedure was used for supporting $Fe_3(CO)_{12}$. Since the adsorption of the iron–carbonyl is slow the mixture was refluxed at 363 K for 1 h. Bimetallic Rh–Fe catalysts were prepared by adsorption of $Fe_3(CO)_{12}$, followed by the adsorption of $Rh_4(CO)_{12}$. The suspension was left under stirring for 2 h. IR analysis of the heptane solution revealed the presence of $Fe(CO)_5$, suggesting that some iron was not completely adsorbed and could be lost. (see Table 1) The prepared samples were heated ($r = 5$ K/min) until 523 K in a fluidized bed, in a stream of H_2 (40 ml/min), to decompose the carbonyls to metals. After 2 h at 523 K the system was cooled to room temperature and the surface of the metals was passivated with 5% O_2 in Ar at 298 K for 15 min. The resulting catalysts were stored in air. The preparation of supported $RhCl_3$ or $Rh(NO_3)_3$ samples was performed by wet impregnation of

ZrO_2 under stirring (18 h) followed by evaporation of water under vacuum and by drying at 383 K for 15 h. Monometallic Fe/ZrO_2 samples were prepared according to the same procedure.

The bimetallic catalysts were prepared according to the previously described wet impregnation technique using a solution of rhodium and iron salts. Only for the chloride precursors a two step wet impregnation has also been performed by supporting $FeCl_3$ on samples previously impregnated with Rh.

All the samples prepared from inorganic salts were calcined at 773 K for 2 h followed by reduction in H_2 stream (40 ml/min) at 523 K for 2 h. All samples were passivated with an oxidizing gas mixture.

Metal analysis was carried out by atomic absorption on a Perkin Elmer 2380 spectrophotometer.

2.2. Catalyst characterization

The supported metals have been characterized by pulse chemisorption of H_2 (5% H_2 in Ar), O_2 (5% O_2 in Ar) at 298 K and titration with H_2 at 373 K of the O_2 chemisorbed at 298 K. Before chemisorption all samples have been pretreated at 523 K in a stream of H_2 (40 ml/min) for 2 h and then in a stream of Ar for 3 h. After this cleaning procedure the catalysts were cooled to 298 K, always in a stream of Ar. The chemisorption temperature of 298 K was chosen on the basis of the literature [11–13]. The titration of chemisorbed oxygen performed at 373, to allow the desorption of water formed during titration [13].

TPR [14] experiments were performed from 298 to 1173 K with a rate of 10 K/min in a stream of H_2 (40 ml/min), using 100–150 mg of catalysts. The hydrogen mixture was purified by an oxy-trap. Before testing, all samples were heated in situ for 1 h at 773 K in a stream of 5% oxygen in argon, followed by cooling at room temperature under the same stream.

The FTIR experiments were performed in situ, after chemical and thermal treatments in the cell, using ultra-high purity gases (Matheson). The spectra (80–100 scans with resolution 2 cm^{-1}) were recorded at room temperature with a Perkin Elmer 1760 instrument equipped with a cryodetector.

2.3. Catalytic activity

Catalytic activity tests were performed in a glass tubular reactor (200 mm long, 8 mm i.d.) immersed in a fluidizes bed of carborundum, externally heated by an oven. The temperature was controlled (± 0.5 K) with a thermocouple immersed in the catalytic bed. The product mixture was analyzed by an on-line GC (Hewlett Packard 5890 A) equipped with two columns and two detectors (Porapak Q to TCD and Porapak R to FID).

About 0.2 g of catalyst diluted with 0.6 g of carborundum (100–200 mesh) was pretreated in H_2 stream at 523 K or at 773 K for 2 h and then cooled at the reaction temperature (493 K). At this temperature the H_2 flow was stopped and the reaction mixture was fed at a rate of 20 ml/min. A transition period of about 4 h was observed for all catalysts. Data were collected 2 h after attaining stationary conditions.

3. Results

3.1. BET, X-ray and chemisorption

The prepared ZrO_2 has a BET surface area of 78 m^2/g and X-ray analysis shows 72% monoclinic and 28% tetragonal phase. The presence of some amorphous ZrO_2 cannot be excluded.

In Table 1 the prepared catalysts and their analytical data are listed. In Table 2 chemisorption and titration data are reported for monometallic Rh samples. The assumed chemisorption stoichiometries are: $H_s/Rh = 1$; $O_s/Rh = 1.5$. The titration stoichiometry results: $H_t/O_s = 2.66$.

From the chemisorption data the diameters of rhodium metal particles determined either with hydrogen (DH) or with oxygen (DO) chemisorption are in good agreement for samples pre-

Table 2
Chemisorption and titration data of monometallic catalysts

	Chemisorption data [a]			Titration data		D_H	D_O
Catalyst	H_s/Rh	O_s/Rh	O_s/H_s	H_t/Rh	H_t/O_s	(Å)	(Å)
Rh(CO)	0.78	1.04	1.33	2.62	2.52	14	16
Rh(N)	0.53	0.74	1.40	1.88	2.54	21	22
Rh(Cl)	0.17	0.64	3.76	1.49	2.33	63	26
[b]	0.48	0.64	1.33	1.49	2.33	22	26

[a] H_s/Rh, O_s/Rh atomic ratio of chemisorbed species; the theoretical value are respectively 1 and 1.5. Therefore the theoretical value of O_s/H_s is 1.5. H_t/Rh, H_t/O_s atomic hydrogen consumption for the titration of chemisorbed oxygen; the theoretical value of H_t/O_s is 2.7.
[b] Samples calcined and washed again to eliminate chloride.

Table 3
Chemisorption data of bimetallic catalysts

Catalysts	Fe/Rh	H_s/Rh	O_s/Rh	H_t/Rh	H_t/O_s	Fe dispersion
Rh(CO)	0.0	0.78	1.04	2.62	2.52	
Rh–Fe(CO)	0.48	0.80	1.86	–	–	100
Rh–Fe(CO)	0.80	0.73	2.12	–	–	95
Rh–Fe(CO)	1.06	0.63	2.25	–	–	90
Rh(Cl)	0.0	0.17	0.64	1.49	2.33	
Rh–Fe(Cl)	0.63	0.11	0.68	1.53	2.25	28
Rh–Fe(Cl)	1.30	0.11	0.82	1.91	2.33	21
Rh–Fe(Cl)	1.42	0.08	0.89	1.94	2.18	27
Rh–Fe(Cl)	3.46	0.04	1.59	3.36	2.11	28
Rh(Cl)	0.0	0.17	0.64	1.49	2.33	
RhFe(Cl)	0.67	0.13	0.69	1.51	2.19	20
RhFe(Cl)	1.27	0.12	0.77	1.75	2.27	17
RhFe(Cl)	1.28	0.10	0.84	1.94	2.31	24
RhFe(Cl)	2.49	0.09	1.40	3.14	2.24	28
Rh(N)	–	0.53	0.74	1.88	5.54	
RhFe(N)	0.62	0.47	0.90	2.10	2.33	26
RhFe(N)	1.40	0.57	1.09	2.47	2.27	14
RhFe(N)	1.90	0.42	1.49	3.34	2.24	31
RhFe(N)	2.00	0.49	1.58	3.40	1.13	30

pared from carbonyl clusters (Rh(CO)) or from nitrate salts (Rh(N)). Moreover the experimental values of H_t/O_s are not far from the theoretical one (2.5 vs. 2.66). As to the sample prepared from chloride, the O_s/H_s value is significantly greater than the theoretical one (1.5) and consequently DH differs greatly from DO. Indeed, after extensive washing to eliminate chloride, this sample behaves similarly to the others.

Chemisorption data suggest that chloride has a strong inhibiting effect on hydrogen chemisorption, while oxygen chemisorption is not affected. Under the same experimental conditions, a sample of iron supported on ZrO_2 prepared and treated as the bimetallic catalysts neither adsorbs hydrogen nor oxygen: this indicates that iron is present in an oxidized form, its reduction occurring only at higher temperatures, as will be shown by TPR data.

In Table 3 the chemisorption data of bimetallic Rh–Fe catalysts are reported: both sets of samples from chloride salts show a low hydrogen chemisorption, indicating the presence of chloride on the surface of the catalysts. Reliable data can be obtained with oxygen chemisorption, that is unaffected by the presence of chloride, as was shown above. These O_s/Rh values indicate a significantly higher dispersion for the samples prepared from carbonyl clusters.

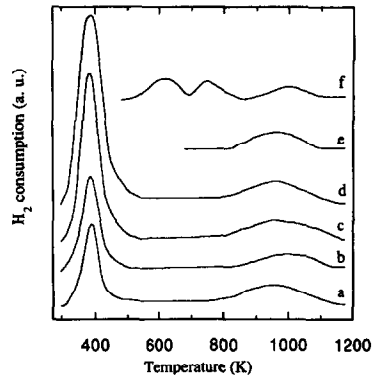

Fig. 1. TPR spectra of Rh–Fe(CO) samples prepared from Rh and Fe carbonyl clusters calcined at 773 K; Fe/Rh atomic ratios: a. 0.0; b. 0.48; c. 0.80; d. 1.06; e. pure ZrO_2; f. Fe(CO).

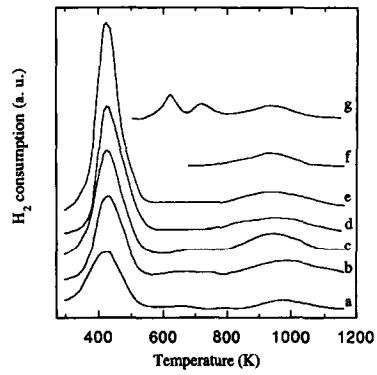

Fig. 2. TPR spectra of RhFe(Cl) samples prepared by co-impregnation of Rh and Fe chloride calcined at 773 K; Fe/Rh atomic ratios: a. 0.0; b. 0.67; c. 1.27; d. 1.28; e. 2.49; f. pure ZrO_2; g. Fe(Cl).

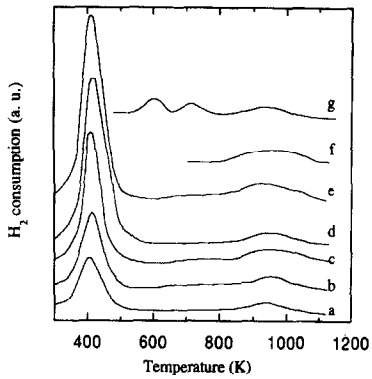

Fig. 3. TPR spectra of RhFe(N) samples prepared by co-impregnation of Rh and Fe nitrate calcined at 773 K; Fe/Rh atomic ratios: a. 0.0; b. 0.62; c. 1.40; d. 1.90; e. 2.0; f. pure ZrO_2; g. Fe(N).

3.2. TPR

In Figs. 1-3 the TPR of samples prepared from carbonyl clusters or salts, using the co-impregnation method, are reported. With Rh/ZrO_2 samples, independently of the precursor used, a hydrogen consumption peak in the range 320–500 K is always present, whose shape is larger in the case of salt precursors than in the case of the carbonyl precursor, showing a greater heterogeneity in Rh dispersion in the former. All Fe/ZrO_2 samples show two hydrogen consumption peaks, the first one at about 600 K and a second one at about 730 K, that have been attributed to a two stage reduction of Fe_2O_3 to Fe^0 through Fe_3O_4 [15]. The peak in the range 820–1140 K, also present on pure ZrO_2, was assigned to the reaction of hydrogen with oxygen atoms present on the surface of zirconia [7]. It has to be pointed out that this peak has a maximum temperature that depends on the preparation procedure of the zirconia and is probably due to the crystalline phase composition.

All bimetallic samples show a hydrogen consumption peak with a maximum in the range 320–500 K, and a second peak in the range 820–1140 K, the former increasing with the content of iron. No iron reduction peaks are present.

These experimental data seem to indicate that in bimetallic samples the whole metal phase reduces in the same temperature range, probably owing to a very close interaction between Rh and Fe causing the catalytic reduction of Fe by dissociated hydrogen spilled from the incipient Rh metal.

All samples, after an oxidation pretreatment (see Experimental), behave similarly in TPR runs, and there are no apparent differences depending on the precursor. The pretreatment was necessary to eliminate the variable amount of CO_2 chemisorbed on the catalysts stored in air and giving rise to a hydrogenation peak in the 500–600 K range during the TPR runs.

3.3. IR

In Fig. 4 are reported the IR spectra of CO adsorbed on the three samples reduced with H_2 at 500 K in static conditions, and evacuated for 10 min at the same temperature.

The curves show an apparently different behaviour. Curve a refers to sample $RhFe(N)_{1.4}$ showing maxima at 2190–2180, 2138, 2062, 2017 cm^{-1} and broad bands at 1900–1850, 1680–1560 cm^{-1}. Curve b shows the spectrum of CO chemisorbed on sample $RhFe(Cl)_{1.28}$: the maxima are at 2187, 2174, 2104, 2038 cm^{-1} and broad bands at 1912–1850 and 1700–1600 cm^{-1}. In curve c the spectrum of CO adsorbed on sample $Rh–Fe(CO)_{0.8}$ is shown: the adsorbing background is

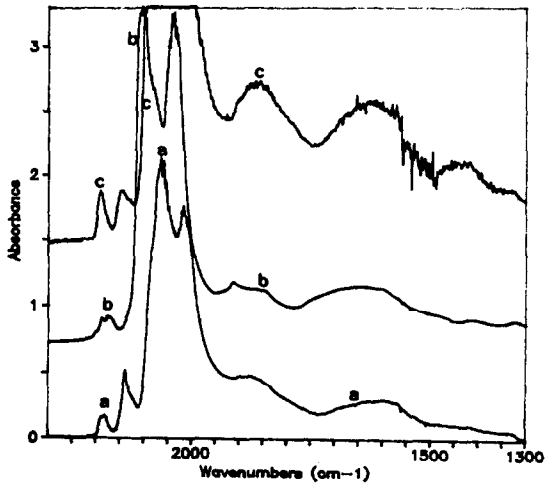

Fig. 4. FTIR spectra of CO adsorbed at 300 K on three samples reduced 60 min and outgassed for 10 min at 500 K; curve a, $RhFe(N)_{1.4}$, $p(CO) = 42$ mbar; curve b, $RhFe(Cl)_{1.28}$, $p(CO) = 32.3$ mbar; curve c, $Rh–Fe(CO)_{0.80}$, $p(CO) = 32.6$ mbar.

very strong (transmittance <1%) and this does not allow to achieve a good resolution. Moreover the envelope of the adsorbed CO bands in the region 2100–1950 cm^{-1} is very intense and out of the capability of detection of the instrument. However weak bands appear at 2190, 2146 cm^{-1} and broad bands are formed at 1865 and 1670–1620 cm^{-1}. This spectrum is very similar to that shown by CO adsorbed on the Rh_4 carbonyls decomposed on ZrO_2 [16] and suggests the same band assignment. The bands at 2146 cm^{-1}, previously assigned to CO weakly chemisorbed on Fe^{x+} ($x \approx 2$) sites for the Fe/ZrO2 system [17], can be correlated to the presence of iron. The band at 2190–2180 cm^{-1} present in all spectra is assigned to CO weakly chemisorbed on coordinatively unsaturated Zr^{4+} sites [16,18].

Curve b shows the formation of two strong coupled bands at 2104 and 2038 cm^{-1}, assigned to $Rh^+(CO)_2$ carbonyl groups [19,20] that easily form and result more stable starting from chloride precursors [21,22]. The weak bands at 2174–2181 cm^{-1} could be tentatively associated to a CO species adsorbed on oxidized Fe^{3+} sites [17], stabilized by the presence of Cl^- on ZrO_2 surface. Only the shoulder at $\approx$2070 cm^{-1} can be correlated to a linear CO adsorbed on reduced Rh species together with the bridged CO species at 1912–1850 cm^{-1} [19]. In agreement with the literature the weak broad doublet bands at 1700–1600 cm^{-1} can be assigned to a bridged CO species, C-bonded on Rh and O-bonded to unsaturated Zr^{4+} or Fe^{x+}; these weak Lewis acid sites [3,16,23] explain the minor decrease of CO stretching frequency ($\approx$200 cm^{-1}) with respect to the Shriver's adducts [3].

Finally, the ex-nitrate sample seems to be the most reduced one, at least as far as the Rh particles are concerned: the strong band at 2062 cm^{-1} may be assigned to CO linearly adsorbed on reduced Rh, whereas the band at 1900–1850 cm^{-1} may be assigned to bridged Rh_2–CO species [18]. The weak broad band at 1680–1560 cm^{-1} is similar to the band at 1700–1600 cm^{-1} of curve b and could be assigned to the same species. The band at 2138 cm^{-1} can be assigned to CO weakly chemisorbed

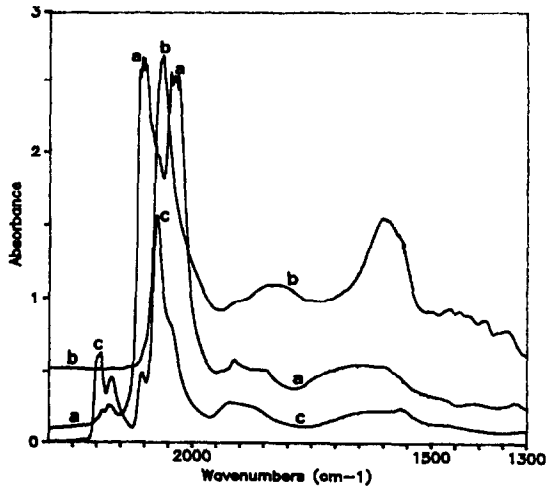

Fig. 5. FTIR spectra of CO and CO + H_2 adsorbed at 300 K on sample $RhFe(Cl)_{1.28}$ after the following treatments: curve a, $H_2/CO = 2$, mixture at $p = 30.6$ mbar adsorbed on the 500 K reduced sample; curve b, after heating the same mixture for 30 min at 500 K; curve c, CO 30.2 mbar adsorbed on the same sample reduced for 60 min and outgassed for 10 min at 773 K.

on Fe^{2+} sites [17]. The band at 2017 cm^{-1} is intermediate between the Rh–CO and Fe–CO [24] stretching frequencies. Tentatively it could be assigned to a linear Rh–CO species surrounded by dispersed Fe atoms. The low intensity and the shift to lower frequency of the bands at $\nu < 2000$ cm^{-1} (bridged Rh_2CO groups) shown in curves a and b may be attributed to the decoration of Rh particle with Fe atoms with formation of bimetallic Rh–Fe ensembles that reduce the number of Rh ensembles able to bind bridged CO [2,21,25].

Fig. 5 illustrates the effect of reduction of the ex-chloride sample by a $H_2/CO = 2$ mixture at 300 and 500 K (curves a and b) and, by comparison, the spectrum of CO on a sample reduced at 773 K (curve c). The spectrum of curve a is nearly identical to that of CO alone adsorbed at 300 K on the same sample, shown in Fig. 4, curve b. Warming for 30 min at 500 K the H_2/CO mixture in the cell (curve b) is however sufficient to eliminate nearly completely the bands at 2104 and 2038 cm^{-1} assigned to $Rh^+(CO)_2$ species with growing of bands at 2062 and 1825 cm^{-1} assigned respectively to CO adsorbed as linear and bridged species on Rh crystals [19]. The reducing effect is demonstrated also by the broad band at 1600–

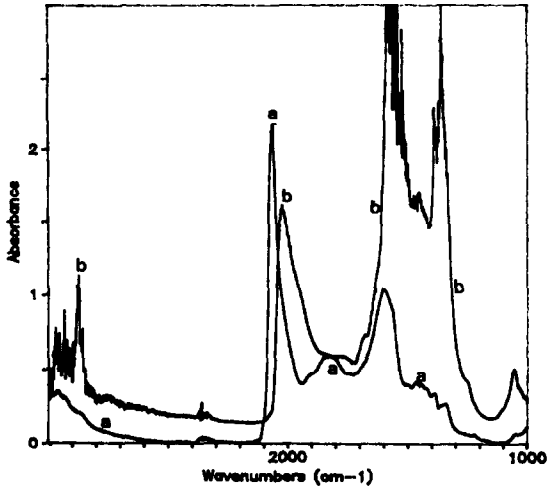

Fig. 6. Comparison between the spectra of H_2/CO mixtures heated at 500 K on samples $RhFe(N)_{1.4}$ and $RhFe(Cl)_{1.28}$: curve a, as curve b of Fig. 5; curve b, spectrum at 300 K of ex nitrate sample reduced at 500 K, after heating 15 min in $H_2/CO = 3$ mixture at $p = 36$ mbar.

1560 cm^{-1}, accompanied by a very strong, broad absorption centred at 3300 cm^{-1}, (not shown in the figure for brevity) and are assigned to H_2O bending and stretching modes perturbed by some HCl formed during reduction. The weak bands at 1458, 1442, 1386, and 1345 cm^{-1} are accompanied by weak bands at 2962, 2932 and 2866 cm^{-1} in the higher region of the spectrum (see Fig. 6) and are assigned to the bending and stretching modes of CH_3 and CH_2 groups in methoxy and ethoxy species.

The spectrum of curve b does not show any band of CO adsorbed on Zr^{4+} sites (that were probably saturated by the water of reaction) and any traces of CO adsorbed on Fe ions. The increase of the band between 1600–1560 cm^{-1} could be correlated not only to H_2O bending but also to an increase of CO species bridging between Rh and an acid centre.

The CO chemisorbed at 300 K on the sample reduced at 773 K (curve c) shows a strong decrease of the coupled bands at 2100 and 2040 cm^{-1} ($Rh^+(CO)_2$) and a relative increase of the band at 2075 cm^{-1}, assigned to CO groups linearly adsorbed on a reduced Rh species probably surrounded by iron sites; in fact, the same frequency is found for CO adsorbed on Rh perturbed by MoO_3 [6].

The bands at 2170 and 2192 cm^{-1} may be assigned to CO adsorbed on Fe^{3+} and Zr^{4+} sites respectively, their high intensity being possibly due to the complete elimination of water at 773 K. The lower intensity of the spectrum of CO adsorbed on Rh (2000–2100 cm^{-1} region) for the sample reduced at 773 K could be attributed to a partial covering of Rh particles by ZrO_2 and/or FeO_x. This hypothesis is supported by the increase of $Zr^{4+}CO$ and $Fe^{x+}CO$ peaks.

In Fig. 6 the spectra of the H_2/CO mixture heated in the cell at 500 K on the ex-chloride (curve a) and on the ex-nitrate (curve b) in the region of C–H stretching (3000–2800 cm^{-1}) and bending (1450–1350 cm^{-1}) modes are compared. The strong bands at 1580–1550, 1350 and 1056 cm^{-1} indicate that on the latter sample the formation of carbonates and formates, that are intermediates in the production of alcohols [3,6,8], is favoured. Moreover the extent of CO hydrogenation is higher, as shown by the lower intensity of the bands at 2022 and 1825 of CO adsorbed on the Rhodium phase. Besides, these bands are shifted to lower frequencies by a diluting effect of H_2 adsorbed on Rh with decreasing of the dipole–dipole coupling of CO overlayers.

3.4. Catalytic activity

The reactivity of all catalysts in the hydrogenation reaction of carbon monoxide was studied at 493 K after pretreatment in H_2 stream at 523 and 773 K. The CO conversion and the product distribution obtained in typical experimental runs are reported in Table 4 for two selected catalysts [Rh(N) and RhFe(N) 1.4].

The following general observation can be made:

carbon dioxide is never found on catalysts prepared from chloride precursor; on all the other catalysts the carbon efficiency to carbon dioxide is independent of the Fe/Rh ratio;

the most evident effect of iron addition is the decrease in the carbon efficiency to higher hydrocarbons (C_4–C_8) while the carbon efficiency to C_1 and C_2 changes very little;

Table 4
Conversion and product distribution data in typical experimental runs

Catalyst	Activation temperature	CO	Product distribution in carbon efficiency (%) [a]							
	(K)	%	CH_4	C_2	C_3	C_{4-8}	MeOH	EtOH	Ox	CO_2
Rh(N)	523	6.0	49.7	2.8	9.2	19.7	1.2	11.9	1.4	4.1
	773	5.3	51.6	2.9	8.1	16.8	1.8	16.7	2.1	–
RhFe(N)1.4 [b]	523	9.2	52.1	2.3	5.6	9.4	3.4	22.1	1.3	3.8
	773	6.0	52.8	3.0	4.9	9.9	3.4	23.6	2.4	–

Reaction conditions: $T_{react.} = 493$ K, $P_{tot} = 101$ kPa, $H_2/CO = 3/1$.
[a] Carbon efficiency = $(n_i A_i / \Sigma n_j A_j)$ where: $n_{i,j}$ = number of carbon atoms in a molecule; $A_{i,j}$ = moles of the product i,j.
[b] Fe/Rh atomic ratio.

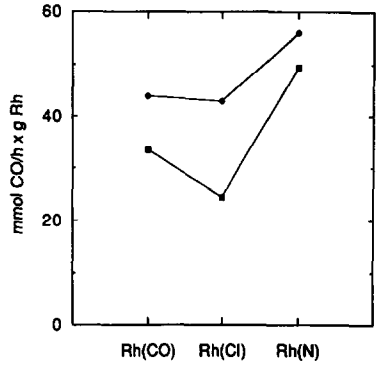

Fig. 7. Rate of CO conversion on unpromoted catalysts prepared from different precursors: activated at 523 K (circles); activated at 773 K (squares).

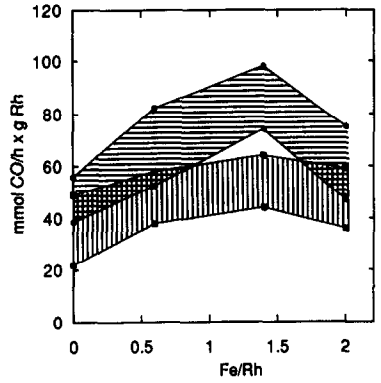

Fig. 8. Rates of CO conversion vs. Fe/Rh atomic ratio. The reported bands refer to the confidence limits of mean reaction rates of different catalysts, independently of the precursor. Activation temperatures: 523 K (circles); 773 K (squares).

a marked increase in the carbon efficiency to methanol and ethanol with increasing iron content is observed, while the carbon efficiency to other oxygenates seems unaffected by the Fe/Rh ratio.

Catalytic tests performed on Fe/ZrO_2 samples show negligible activity (CO conversion <1%) only for samples reduced at 773 K.

Due to the small differences among the various sets of activity data of bimetallic catalysts (sometimes in the range of the experimental error) instead of presenting individually all the kinetic results it has been preferred to plot the band of confidence limits of the mean values. In Fig. 7 the rate of CO conversion (mmol CO/h g Rh) on monometallic catalysts from the various precursors is plotted: the activities of the four catalysts are not significantly different, however the catalysts pretreated at high temperature have a lower activity than those pretreated at low temperature.

In Fig. 8 the confidence limits of the mean values of CO conversion on the various catalysts independently of the precursor vs. the Fe/Rh ratio

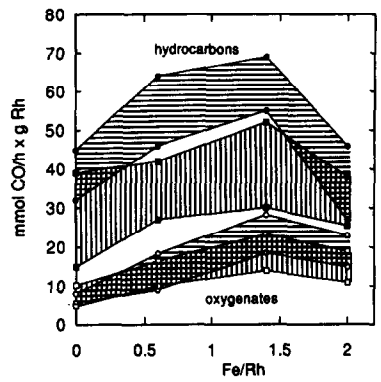

Fig. 9. Rates of CO conversion to total hydrocarbons (solid symbols) and to total oxygenates (open symbols) vs. Fe/Rh atomic ratio. The reported bands refer to the confidence limits of mean reaction rates of different catalysts, independently of the precursor. Activation temperatures: 523 K (circles); 773 K (squares).

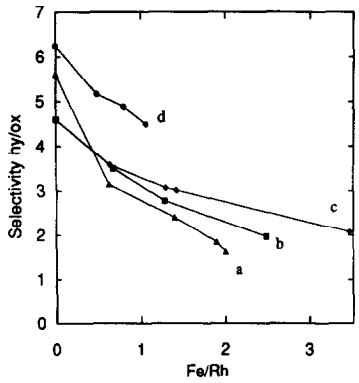

Fig. 10. Selectivity ratio between total hydrocarbons and total oxygenates formation rates vs. Fe/Rh atomic ratio. a: RhFe(N); b. RhFe(Cl); c. Rh–Fe(Cl); d. Rh–Fe(CO).

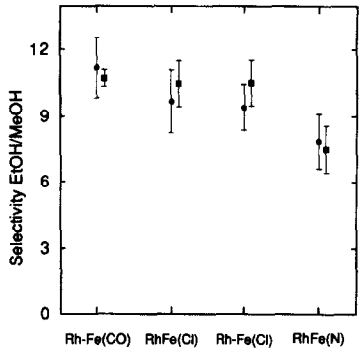

Fig. 11. Selectivity ratio between EtOH and MeOH formation rates. For each set of catalysts the mean value with the relevant standard deviation is reported. Activation temperatures: 523 K (circles); 773 K (squares).

is reported. The upper band refers to the catalysts activated at 523 K and the lower at 773 K.

In Fig. 9 are reported the confidence bands for the mean values of the rate of total hydrocarbon and of total oxygenated compounds on catalysts activated at 523 K and at 773 K. It seems that the effect of iron is slightly greater on the rates of hydrocarbons than oxygenates formation. In order to evidence the effect of Fe on the selectivity of the reaction, in Fig. 10 the ratio between the total hydrocarbon formation rate and the total oxygenate formation rate vs. the Fe/Rh ratio is reported: indeed in all cases Fe promotes the formation of oxygenates.

To investigate whether Fe promotes the selective formation of one of the lower alcohols, the ratios between the rate of formation of ethanol and methanol vs. the Fe/Rh ratios have been reported in Fig. 11. For each set of catalysts the rate ratios change randomly with Fe/Rh therefore only the confidence limits bands of mean values of the rate ratios are reported. The figure indicates that for the whole set of the catalysts, either those activated at 523 K or those activated at 773 K, no significant variation in the ratio of ethanol to methanol formation rate is evident.

4. Discussion

The presence of a strong peak in TPR spectra of all bimetallic catalysts and the absence of any signal of reduction of iron indicate that in H_2 atmosphere Rh is able to reduce iron oxide at the same temperature of Rh reduction (≈ 373 K) forming bimetallic Rh–Fe ensembles [9]. Since normally the reduction of Fe oxides occurs at higher temperature (see Fig. 1) this observation may indicate that, during rhodium reduction, the adsorbed hydrogen atoms have a very high rate of spillover so that they reduce iron oxide at the same temperature of Rh reduction. This explanation is in line with that one proposed by Garten for the system Pd–Fe supported on silica [26]. Indeed not all the iron is reduced as IR spectra show a weak Fe^{n+}–CO band ($n = 2, 3$) in the range 2138–2174 cm^{-1}.

An analysis of oxygen chemisorption data seems to indicate that only on catalysts prepared by carbonyl clusters iron is highly dispersed while in the other cases large iron particles are present. The dispersion of iron can be calculated by assuming that the H_s/O_s ratio for monometallic Rh/ZrO_2 is the same also for each set of bimetallic catalysts and does not depend on the amount of iron present, that is, this ratio is a constant, independently of the presence of iron. This allows to calculate the excess of oxygen chemisorbed on iron containing samples and therefore to calculate the dispersion of iron relative to the theoretical value of oxygen chemisorbed on the bases of the iron content.

These values are reported in the last column of Table 3. It results that on samples prepared by

salts the amount of iron that can be titrated at room temperature is, at the maximum, one third of the total iron present indicating that iron is present mainly as large particles or in a partially oxidized state (e.g. Fe^{2+}).

In fact IR spectra revealed the presence of Fe^{n+} ions not easily reducible and stabilized by thermal treatment at 773 K. We suggest that these are isolated iron atoms on ZrO_2 surface, stabilized in oxidized state by surface hydroxyl groups. A quite narrow band at 3660 cm^{-1} remains in fact in the spectrum after this treatment (data not shown for the sake of brevity): it could be attributed to OH groups bound to zirconia but also to an isolated ferrous site. For ex-chloride or ex-carbonyl samples there is no evidence of any interaction between rhodium particles and iron, while in the case of ex-nitrate samples, Fig. 4, curve a, the CO band at 2017 cm^{-1} indicates the presence of an interaction between Rh particles and iron. However it is not possible to exclude a partial coverage of rhodium particles by iron as indicated by the decrease of hydrogen adsorption by increasing the amount of the Fe/Rh ratio (Table 3).

Fig. 7 indicates that the reaction rate of CO hydrogenation (mmol CO/h g Rh) change little with the precursor used. Rates have been expressed with respect to the weight of Rh present, in order to make a comparison between the monometallic and the bimetallic catalysts. In fact, in the case of bimetallic catalysts it is impossible to determine, without arbitrary assumptions, the number of surface active sites and to distinguish between the role of rhodium and that of iron. On the other hand the TOF (molecules of CO/s atom Rh) for monometallic catalysts changes from 1.6×10^{-3} in the case of catalysts prepared from rhodium carbonyls to 4.5×10^{-3} in the case of nitrate precursor, thereby reflecting the estimated Rh surface sites as determined by hydrogen chemisorption.

The effect of iron on the reaction rate is complex: for low Fe/Rh ratios (<1.5) iron increases the reaction rate, but for higher values there is a significant decrease. This trend is the same also for the catalysts activated at high temperature, although with lower reaction rates. In all cases iron does not significantly change the reaction rates. This can be due to the fact that only a small fraction of iron, decorating or at the border line of rhodium particles, is active in the CO reaction. Isolated Fe^{n+} ions or large iron particles are not active under the experimental conditions used, the latter conclusion being supported by the activity test performed on Fe/ZrO_2 samples. Increasing the Fe content increases the fraction of surface rhodium atoms covered by iron and no longer available for a direct interaction with CO.

Promotion effects of iron on supported noble metals have been observed by various authors [9,10,27–32]. Ichikawa [25], following a model proposed by Yermakov [32] and Prins [33] to explain the role of Re in Pt–Re/Al_2O_3 catalysts, suggests that in catalysts with low Fe/Rh ratio (<1), most of the iron atoms are present as Fe^{3+} and are located at the metal–support interface forming Rh–Fe–SiO_2 bonding. When the Fe/Rh atomic ratio is increased, or in reducing reaction conditions, the fraction of Fe^0 relative to Fe^{3+} increases. EXAFS analysis [33] showed that the excess Fe atoms, mostly as Fe^0, are more likely to be found on the surface of a Rh metal particle.

Indeed the IR spectrum of Fig. 5, curve b, shows that under reaction conditions no free Fe^{3+} species are present and therefore the only possible promotion role may be due to Fe^0 on Rh particles. The shoulder at 2000–1950 cm^{-1} (see also Fig. 6) may account for CO adsorbed on such Fe^0 sites. Following the model proposed by Ichikawa [10,34] we suggest that Fe^{x+} ions contiguous to Rh atoms may give rise to a two-centre activation site on which CO can be adsorbed having C coordinated to Rh and O coordinated to adjacent Fe. Under reaction conditions the Fe^{x+} ions are reduced to Fe^0, but since Rh is more electronegative than Fe, atoms of Fe on the surface of Rh particles may have slightly acidic properties.

Depending on the surface environment, the Rh–CO–Fe species may either dissociate to Rh–C and FeO or insert a hydrogen or an alkyl group with formation of an acyl species.

Since we have proved that under the reaction conditions used, iron alone is not active, the addition of Fe on Rh/ZrO_2 catalysts produces two opposing effects:
it reduces the number of Rh atoms available for CO and hydrogen adsorption;
it increases the number of doubly bonded CO and favours the formation of oxygenated products.

Even at high values of Fe/Rh ratio (>1.5) when the negative effect of the covering of the Rh particles dominates, the rate of formation of oxygenates is still higher than on monometallic samples, as shown by Fig. 9.

Nevertheless the Lewis acid properties of Fe, as ion surrounding the Rh^0 particles and as the intermetallic Rh–Fe cluster in reaction conditions induced by the small difference in electronegativity with rhodium, must be weak and therefore the effect of iron is not comparable with that of stronger Lewis acids, such as Mo^{x+} or Zr^{4+}, as has been shown in a previous paper [7].

In conclusion, iron promotes the activity and the selectivity to oxygenated products in Rh/ZrO_2 catalysts when present in small quantity (Fe/Rh <1.5), while it decreases the activity only when present in larger amount. However, only the fraction of iron in direct contact with Rh has some role in the reaction and behaves like a weak Lewis acid centre promoting the formation of doubly bonded CO, that is the determining step in the formation of oxygenated products.

Acknowledgements

The financial support from MURST is gratefully acknowledged. Thanks are expressed to Miss T. Fantinell (University of Venice) for skilful technical assistance.

References

[1] C. Dell'Agnol, A. Gervasini, F. Morazzoni, F. Pinna, G. Strukul and L. Zanderighi, J. Catal., 96 (1985) 106.
[2] A. Benedetti, A. Carimati, S. Marengo, S. Martinengo, F. Pinna, R. Tessari, G. Strukul, T. Zerlia and L. Zanderighi, J. Catal., 122 (1990) 330.
[3] M. Ichikawa and T. Fukushima, J. Phys. Chem., 89 (1985) 1564.
[4] W.M.H. Sachtler and M. Ichikawa, J. Phys. Chem., 90 (1986) 4752.
[5] L.E.Y. Nonneeman, A.G.T.M. Bastein and V. Ponec, Appl. Catal., 62 (1990) 23.
[6] E. Guglielminotti, E. Giamello, F. Pinna, G. Strukul, S. Martinengo and L. Zanderighi, J. Catal., 146 (1994) 422.
[7] F.G.A. van der Berg, J.H.E. Glezer and W.M.H. Sachtler, J. Catal., 93 (1985) 340.
[8] M. Ichikawa, T. Fukushima and K. Shikakura, Proc. 8th ICC (Berlin), Vol. 2, Verlag Chemie, Dechema, 1984, p. 69.
[9] M. Ichikawa, A. Fukuoka and T. Kimura, in M.J. Phillips and M. Ternan (Eds.), Proc. 9th ICC Calgary, Vol. 2, 1988, p. 569.
[10] A. Boffa, C. Lin, A.T. Bell and G.A. Somorjai, J. Catal., 149 (1994) 149.
[11] H.C. Yao, S. Japar and M. Shelef, J. Catal., 50 (1977) 407.
[12] S. Fuentes and F. Figueras, J. Catal., 61 (1980) 443.
[13] S. Ard, E. Wanke and N.A. Dougharty, J. Catal., 24 (1972) 347.
[14] Y. Kobori, H. Yamasaky, S. Nalto, T. Onishi and K. Tamaru, J. Chem. Soc., Chem. Commun. (1981) 92.
[15] A. Benedetti, G. Fagherazzi, F. Pinna, G. Rampazzo, M. Selva and G. Strukul, Catal. Lett., 10 (1991) 215.
[16] E. Guglielminotti, J. Catal., 120 (1989) 287.
[17] E. Guglielminotti, J. Phys. Chem., 98 (1994) 4884.
[18] E. Guglielminotti, Langmuir, 6 (1990) 1555
[19] L.H. Dubois and G.A. Somorjai, Surf. Sci., 91 (1980) 514.
[20] F. Solymosi and J. Sarkany, Appl. Surf. Sci., 3 (1979) 68.
[21] S.S.C. Chuang, G. Srinivas and A. Mukherjee, J. Catal., 139 (1993) 490.
[22] G. Srinivas and S.S.C. Chuang, J. Phys. Chem., 98 (1994) 3024.
[23] M. Ichikawa, Adv. Catal., 38 (1992) 283.
[24] U. Seip, M.C. Tsai, K. Christmann, J. Kuppers and G. Ertl, Surf. Sci., 139 (1984) 29.
[25] M. Ichikawa, T. Fukushima, T. Yokoyama, N. Kosugy and H. Kuroda, J. Phys. Chem., 90 (1986) 1222.
[26] R.L. Garten and D.F. Ollis, J. Catal., 35 (1974) 232.
[27] M. Bhashin, W.J. Bartley, P.C. Ellgen, and T.P. Wilson, J. Catal., 54 (1978) 120.
[28] T. Fukushima, H. Arakawa and M. Ichikawa, J. Phys. Chem., 89 (1985) 4440.

[29] T. Fukushima, K. Araki, and M. Ichikawa, J. Chem. Soc. Chem. Comm. (1986) 148.
[30] T. Fukushima, Y. Ishii, Y. Onda and M. Ichikawa, J. Chem. Soc. Chem. Comm. (1985) 1752.
[31] D.C. Koninsberger, C.P.J.H. Borgmans, A.M.J. van Elderen, B.J. Kip, and J.W. Niemantsverdriet, J. Chem. Soc., Chem. Commun. (1987) 892.
[32] Y. Yermakov, Catal. Rev.-Sci. Eng., 13 (1976) 77.
[33] T. Huizinaga and R. Prins, J. Phys. Chem., 87 (1983) 173.
[34] A. Fukuoka, M. Ichikawa, J.A. Hriljac and D.F. Shiver, Inorg. Chem., 26 (1987) 3643.